International Journal of Engineering

Journal Homepage: www.ije.ir

Life Estimate of a Compressor Blade through Fractography

E. Poursaeidi *, M. Sanaieei, H. Bakhtyari

Department of Mechanical Engineering, University of Zanjan, Zanjan-45371-38791

P A P E R   I N F O

A B S T R A C T

Failure analysis of fractured components provides some information about the causes and conditions of fracture. Fractography is an indispensable part of the failure analysis as it is usually the only means by which the failure mechanism can be established. By using fractography, some information such as component's life, values of the stress intensity factor and the applied stress can be calculated. In this paper, the results of categorized investigations and tests such as chemical analysis and fractography of a failed compressor blade of a Frame 6 type gas turbine engine have been presented. The results showed that the source of initial cracks on the blade is corrosion pitting on the surface of the blade. The failure mechanism is high cycle fatigue. Crack growth rate has been calculated from striation spacing and has been compared with the numerical solution. The stress intensity factor range and the applied stress range have also been calculated and compared with numerical results. Fractographic analysis and numerical computations are consistent with each other.

1. INTRODUCTION

Failure analysis is the process of collecting and analyzing data to determine the cause of a failure. It relies on collecting failed components for subsequent examination of the cause or causes of failure using a wide array of methods, especially microscopic and spectroscopic inspections [1]. More than 80% of failure accidents are due to fatigue resulting from incorrect designs of machine parts. Failure analysis provides valuable information on similar failure accidents that may be useful for improving existing designs or developing new products [2]. Usually, the failure analysis of broken parts consists of quantitative and qualitative methods. Qualitative methods include the use of the naked eye, metallurgical microscope, etc. Quantitative methods use SEM (Scanning electron microscope), X-ray diffraction, etc. Among the quantitative methods, fractography by SEM can estimate the stress amplitude of fatigue failure parts by using the relation between striation spacing and the stress intensity factor range. Fractography is the science of studying the fracture surface in order to determine the source of fracture and relationship between the mode of crack propagation and the microstructure of the material

[3]. One of the basic tasks of fractography is the reconstitution of fatigue crack growth history from the morphology of the crack surface. The merits of all methods consist of relating the morphology of crack surface to the crack growth rate [4]. As a basis for expressing this relation, striation spacing analysis may also be used (among many other methods).

The striation counting for estimating fatigue crack growth life was suggested many years ago. Several authors believe that there is a one-to-one correspondence between striation and stress cycle [5-7]. Other researchers believe that there is not such a simple relationship between striation counting and the crack growth rate, especially at low amplitude of stress intensity factor (crack initiation, region I of fatigue life) [8]. Therefore, it is not possible to determine the number of load cycles which occurred during the initiation stage. However, this relationship is established in the region II of fatigue crack growth life (intermediate value of stress intensity factor).

Hoeppner and Krupp [9] proposed some equations for estimating fatigue life based on fractographic data. Katsuaki [10] has presented a method for estimating service load from striation's width and height. DeVries et al. [11] discussed about striation counting accuracy and its advantages and disadvantages. Yang et al. [12] present a statistical model of quantitative relationship

* Corresponding Author Email: *epsaeidi@znu.ac.ir* (E. Poursaeidi)

between striation spacing and fatigue crack growth rate. Nedbal et al. [13] suggest a new model for estimating fatigue life from striation spacing with considering idle cycles (those cycles which don't create a striation). In Nedbal's proposed model, the crack growth rate is equal to striation spacing multiplied by a coefficient, D(S). This coefficient is a function of idle cycles, spatial dispersion of local directions of the crack growth and influence of crack growth micromechanisms other than the striating one (e.g. ductile fracture, quasi-cleavage, decohesion & cleavage of inclusions, etc.). The coefficient D(S) can be obtained by some experimental procedures [13]. Also, Nedbal et al.[14] proposed a textural fractographic model for life estimate of those components that fail in a mechanism other than fatigue. Troshchenko and Prokopenko [15] investigated the effect of various factors (such as corrosive environment) on the fatigue strength of gas turbine compressors blades through some experimental procedures. S.P. Lynch studied the effect of environment on fatigue striations, their spacing and their quality [16]. Ruckert et al. proposed an equation for estimating the load ratio (R) from striation width (s) and height (H) [17].

In this paper, fatigue life will be estimated based on the relationships between striation spacing and crack growth rate. The power plant under investigation in this paper is established in a coastal area in south IRAN. It is equipped with four 40 MW Frame 6 type gas turbine engines which are named GTG A, B, C and D that have been installed in less than a decade. GTG D was tripped by a violent sound due to compressor failure. GTG A and B had failed earlier with similar catastrophic events.

2. MATERIAL AND METHOD

2. 1. Properties of Compressor Blade The working time of the GTG D compressor was 26780 hours. Preliminary observations such as failure of a moving blade in the 1st row and damages on other moving and stationary blade indicate that the incident occurred in the GTG D compressor was similar to the previous events on the other compressors of the unit. Figure 1 shows the following failure status of the incident at the compressor inlet. In this figure, the remaining part of the broken blade on the rotor can be observed. Analysis and visual inspection indicated that a moving blade of the 1st row was first destroyed (broken). Other stationary and moving blades were observed with damage by solid objects and particles, which originated from the destroyed blades of the 1st row.

Visual inspection and fractography of blades were done by using a light microscope, stereo microscope and scanning electron microscope (SEM) in 100× - 10000× magnifications. Chemical composition of the blade was obtained by EDAX microprobe in Shahryar Turbine Components Co. Tests show the material of the

blade to be AISI Custom 450 (GTD 450) which is a precipitation hardened, martensitic stainless steel [18] and its composition is presented in Table 1. This material provides increased tensile strength without sacrificing stress corrosion resistance. Substantial increases in the high-cycle fatigue and corrosion fatigue strength are also achieved with this material. Superior corrosion resistance is also achieved due to its higher concentration of chromium and molybdenum [18].

EDAX chemical analysis using SEM in pitting locations showed that there are many non-structural elements such as S, Cl and Na. It should be noted that no surface cleaning was done at this stage for chemical analysis. The results are shown in Figure 2.

Figure 3 shows the surface of the fractured blade. In the fracture surface, fatigue fracture features (such as beach marks) can clearly be observed. Figure 3 also illustrates the fatigue area and the final fracture region with an angle of 45° (in trailing edge). Figure 4 shows that two semi-elliptical cracks are recognized and imply that the cracks extended from two different crack fronts. Also, beach marks are evident in this figure.
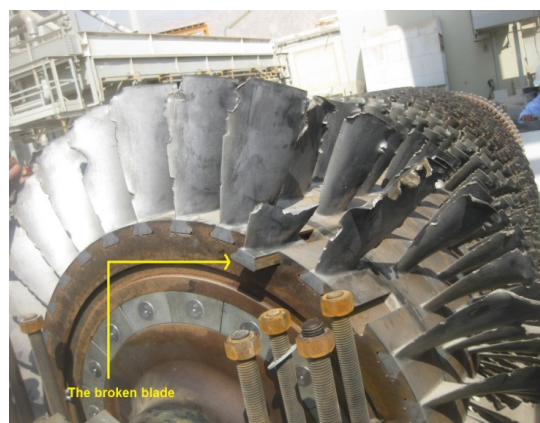

Figure 1. The fractured blade and other damaged blades.

TABLE 1. Results of material chemical analysis of the 1st row compressor blade

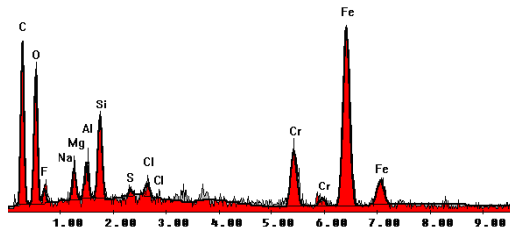| Element	Wt% (experiment)	Wt% (reports of the manufacturer [18])
Ni	6.43	6.3
Cr	15.17	15.5
Mo	0.79	0.8
C	0.027	0.03
Mn	0.6	0.4
Cu	1.48	1.5
Fe	Balance	Balance

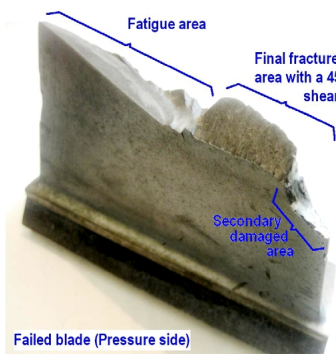**Figure 2**. Chemical analysis of the broken blade

Figure 3. Fracture surface of the GTG D compressor's 1st row moving blade
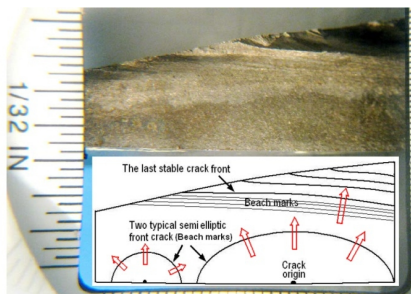

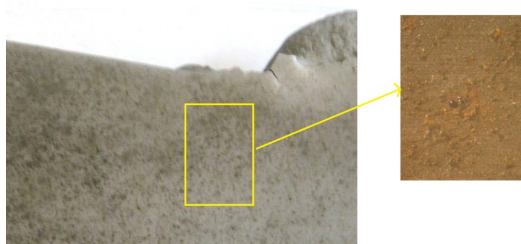**Figure 4.** Fracture surface of blade

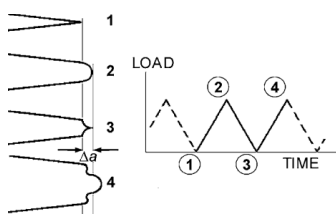**Figure 5.** Brown spots on the pressure side of the blade

Figure 6. Striation forming [13]

Airfoil surface is covered with tiny brown spots that represent signs of pitting. Density of these spots in the pressure side of the airfoil is more than in suction side (Figure 5).

2. 2. Theoretical Background   Fatigue in materials subjected to repeated cyclic loading can be defined as a progressive failure due to crack initiation (stage I), crack growth (stage II), and crack propagation (stage III) or instability stage. In general, fatigue is a form of failure caused by fluctuating or cyclic loads over a short or prolong period of time. Therefore, fatigue is a time-dependent failure mechanism related to microstructural features[13].

In the electron microscope examination of fatigue-fracture surfaces, the most prominent features found are patches of finely spaced parallel marks, called fatigue striations. The fatigue striations are oriented perpendicular to the microscopic direction of crack propagation [19].

The first communication about striations is usually attributed to Zappfe and Worden. Since then (1951), the mechanism of striation forming has been described by many authors and models. The most convenient model for fractographic interpretation is the simplified diagram of François et al. in Figure 6, describing the formation of the first striation as the fatigue crack passes from stage I to stage II of propagation [13].

As mentioned before, many authors have carried out investigations to find a relationship between striation spacing and fatigue life. The process of measuring striation spacing is shown in Figure 7.

In Figure 7, the big arrow is the macroscopic crack growth direction and the small arrows are local crack growth directions.

Fracture Equation (1) is derived from the relation between striation spacing (S) and crack propagation rate (da/dN) and the relation between crack propagation rate (da/dN) and the stress intensity factor range (ΔK):[2]

$$S = 9.4(1 - v^2)(\Delta K/E)^2 \tag{1}$$

where v and ΔK represent Poisson's ratio and the range of the stress intensity factor, respectively. The mechanical properties of GTD 450 are presented in Table 2.

TABLE 2. Mechanical properties of GTD 450 [20]

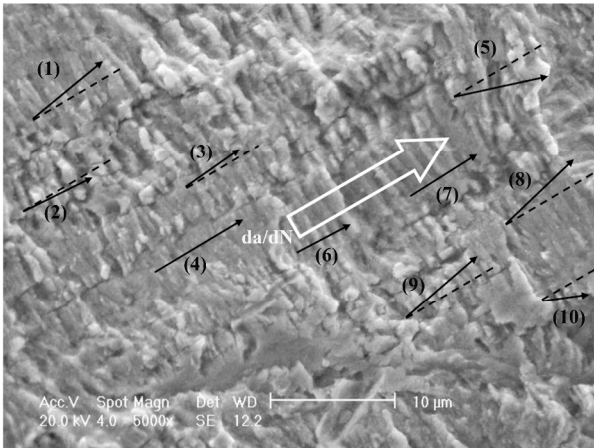| Property	Magnitude
Material	GTD 450
Density, ρ(kg/m^3)	7800
Modulus of Elasticity, E(GPa)	200
Poisson's Ratio, v	0.29
Yield Stress, σ_y(MPa)	814
Fracture Toughness, K_{Ic}(MPa.m$^{1/2}$)	110

Figure 7. SEM (5000x) of middle section of big semi-elliptical; the big arrow is the direction of macroscopic crack growth, black arrows are directions of local crack growth direction and dashed lines are in direction of macroscopic crack growth in order to measuring ϑ_p in Equation (5).
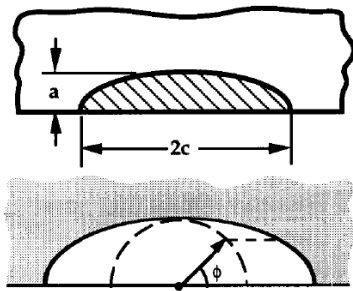

Figure 8. An elliptical crack [1]

Another empirical relation that can be used to relate the striation spacing (S) and stress intensity factor range (ΔK) is presented by Bates and Clark [21]:

$$\Delta K = E \sqrt{S/6} \qquad (2)$$

After calculation of ΔK, the applied stress range $\Delta\sigma$ can also be determined. For elliptical cracks [1]:

$$\Delta K_I = \lambda_s \Delta\sigma \sqrt{\pi a/Q}\, f(\phi) \qquad (3)$$

where

$$\lambda_s = \left[1.13 - 0.09\left(\frac{a}{c}\right)\right]\left[1 + 0.1\left(1 - \sin\phi\right)^2\right]$$

$$Q = 1 + 1.464\left(\frac{a}{c}\right)^{1.65};$$

$$f(\phi) = \left[\sin^2\phi + \left(\frac{a}{c}\right)^2\cos^2\phi\right]^{1/4}$$

a, c and Φ are shown in Figure 8.
For calculating the average value of striation spacing in Figure 7, the following equation can be used [13]:

$$S = \frac{1}{k}\sum_{i=1}^{k} S_{p_i}\cos\vartheta_{p_i} \qquad (4)$$

where p=1,2,..,k is the number of lines, $S_p = l_p/n_p$ is the average striation spacing on p^{th} line, l_p is the length of the pth line, n_p is number of striations on the line l_p and ϑ_p is the angle between p^{th} line and the macroscopic crack growth direction [13].

The fatigue crack growth rates can be determined from the fracture surface studies using scanning electron microscopy (SEM). The crack growth rate is calculated using [6]:

$$\frac{da}{dN} = \frac{1}{magnification}$$
$$\times \frac{\text{distance on the fractograph}}{\text{striation count /unit distance on the fractograph}} \qquad (5)$$

3. RESULTS AND DISCUSSIONS

3. 1. Fratography   Visual inspections show that the crack origins are two pits on the pressure side of the blade (Figures 4 and 9). The average value and measured values for striation spacing in different positions in Figure 7 are presented in Table 3.

Near the final fracture zone, where the area of the blade becomes gradually smaller, stresses are very high and as a result of this high stress, secondary cracks have appeared. Figure 10 shows secondary cracks near the final fracture zone.

Figure 9. A view of the fractured bled surface with a pit on the pressure side.

Figure 10. Presence of secondary cracks near the final fracture zone (high stresses)

TABLE 3. Measured values for striation spacing in different positions in Figure 7

Line(p)	$S_p(\mu m)$	Φ_p(degree)
1	1	5
2	1.11	4
3	0.95	2
4	10.2	13
5	0.85	0
6	0.85	0
7	0.76	0
8	0.8	5
9	0.8	2
10	0.7	19
S (average)=0.876 μm		

Presence of corrosion pits means that the initiation stage of fatigue crack growth life has not occurred. So it can be concluded that the crack is entered directly into the second stage of fatigue crack growth life. Thus, the simple relations between striation spacing and crack life, which are applicable in the second stage of fatigue life, can be used here.

Comparison of the areas of the fatigue region and the final fracture region in the fracture surface indicates that the final fracture has a small area in the fracture surface, so it can be concluded that the applied stress was low and the fracture mechanism is High Cycle Fatigue (HCF).

3. 2. Calculation Results   The crack growth direction is shown in Figure 7 by the yellow arrow. For calculating the stress intensity factor range and the crack growth rate from Equations (1)-(3), striation spacing was measured using SEM pictures (Table 3).
By using Equation (1) and with an average striation spacing of $S = 8.76 \times 10^{-4}$ mm,

$$8.76 \times 0^{-4} = 9.4(1 - 0.29^2)(\Delta K / 200 \times 10^3)^2 \rightarrow$$
$$\Delta K = 63.81 MPa\sqrt{m}$$

Calculation of ΔK from Equation (2) and with the same average striation spacing yields:

$$\Delta K = 200 \times 10^3 \sqrt{\frac{8.76 \times 10^{-7}}{6}} = 76.44 MPa\sqrt{m}$$

Since the calculated range of ΔK are not in the low amplitude [8], simple relationships between striation spacing and fatigue life can be used.

By using Equation (4), one can estimate the crack growth rate as:

$$\frac{da}{dN} = \frac{1}{5000} \times \frac{5.6mm}{12} = 0.0926 \, \mu m/cycle$$

The measured values for initial and final lengths of the crcak is $a_0 = 0.5mm$ and $a_f = 10mm$. Therefore, by integrating the above equation, the life is estimated at 102592 cycles.

By this amount of crack growth rate and by using the Paris law, the effective stress intensity range can be calculated as [1]:

$$\frac{da}{dN} = 1.34 \times 10^{-13} (\Delta K_{eff})^{3.45} \tag{6}$$

so

$$\Delta K_{eff} = 49.27 MPa\sqrt{m}$$

The stress ratio can be obtained by using the following relation as [6]:

$$\Delta K_{eff} = U \Delta K \tag{7}$$

Although U may be taken as a complicated function varying from cycle to cycle and from one loading condition to another, for conventional fatigue programs U can be assumed to be quite simple and a function of R only [6]

$$U = 0.618 + 0.365R + 0.139R^2 \tag{8}$$

From Equations (7) and (8) and by using the value of $\Delta K = 63.81$, the value of stress ratio is equal to R=0.4, which is consistent with experimental results.
For calculating $\Delta\sigma$ from Equation (3), the following values λ were obtained: Φ=90°, a=0.56 cm and c=0.88 cm. By using these values, one can calculate the stress range as:

$$\lambda_s = \left[1.13 - 0.09\left(\frac{0.56}{0.88}\right)\right]\left[1 + 0.1(1 - \sin 90)^2\right] = 1.07$$

$$Q = 1 + 1.464\left(\frac{0.56}{0.88}\right)^{1.65} = 1.69$$

$$f(\phi) = \left[\sin^2 90 + \left(\frac{0.56}{0.88}\right)^2 \cos^2 90\right]^{1/4} = 1$$

$$\Delta\sigma = \frac{\Delta K_{eff}}{\lambda_s \sqrt{\pi a/Q} \, f(\phi)} = \frac{\Delta K_{eff}}{0.154} = 254.30 MPa$$

To verify the accuracy of calculations, the results were compared with numerical analysis in FRANC 3D [22]. According to the fractography of the fracture surface, the exact locations and dimensions of cracks were measured. After that, cracks were inserted into the model in FRANC3D (Figure 11). By applying the boundary conditions and the applied stress to the model, analysis was done and cracks were grown until the final fracture.

Figure 13 shows the changes of K along the crack front in different steps. The calculated value of ΔK is for the stage of coalescence of two cracks (see Figure 12) and is in the range of numerical solution of K (see Figure 13-c). Figure 13 shows the computed life by numerical solution with different models. The

calculated life by fractography which is shown by the dashed line is in good agreement with numerical solutions for two-crack condition.

During the crack growth stage, with each incremental growth of crack length, the value of ΔK increases. At the time of coalescence of two cracks, crack length increases spontaneously, and as a result, the value of ΔK approaches to its ultimate limit (ΔK$_{Ic}$). This increase in the ΔK value occurs while in the case of one crack, more steps should be passed to achieve this amount. Therefore, the fatigue life in two-crack condition is less than one-crack state and numerical analysis confirms this issue (see Figure 14).

4. CONCLUSSION

❖ Fractography of the fractured surface indicates that the crack origins are two pittings on the pressure side.Chemical analyses confirm the presence of corrosive elements.
❖ Failure mechanism is High Cycle Fatigue (HCF).
❖ The crack is entered directly into the second stage of fatigue crack growth life.
❖ The calculated crack growth rate using empirical relationships was 0.15μm/cycle, which is consistent with numerical solutions.
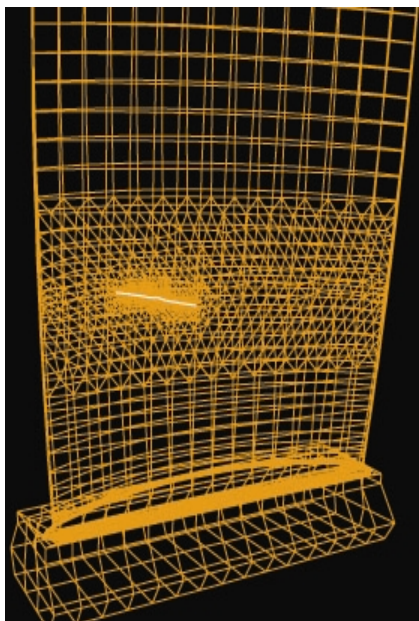❖ The calculated value of ΔK for the stage of joining two cracks is consistent with the numerical solution results.

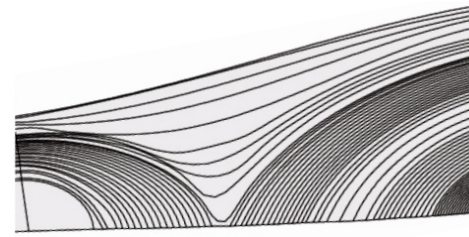**Figure 11.** The bigger crack have been inserted to the model [22].

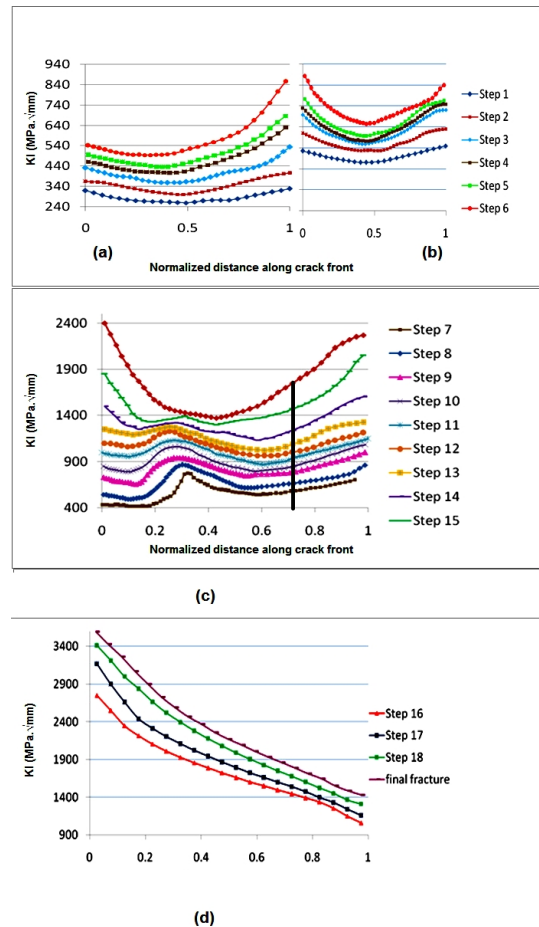**Figure 12.** Coalescence simulation in FRANC3D [22]

Figure 13. SIFs Curve in a) pre-coalescence for small crack b) pre-coalescence stage for big crack c) coalescence stage d) post-coalescence stage [22]
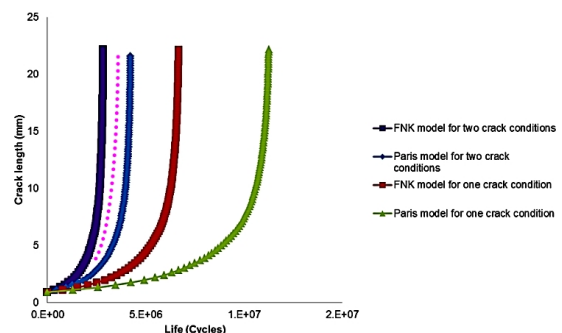

Figure 14. Crack growth curves [22]

5. REFERENCES

1.   Anderson, T. L. C., "Fracture mechanics: fundamentals and applications", *CRC Press*, (1995).
2.   Lee, D., Cho, S. and Joo, W., "An estimation of failure stress condition in rocker arm shaft through FEA and microscopic fractography", *Journal of Mechanical Science and Technology.* Vol. 22, (2008), 2056-2061.
3.   Shukla, A., "Practical fracture mechanics in design", *Marcel Dekker*, (2005).
4.   Lauschmann, H., Bendarik, P., Sekeresova, Z. and Benes, M., "Fractal image feature vectors with applications in fractography", *Image Anal Stereol*. Vol. 27, (2008), 63-71.
5.   Connors, W.C., "Fatigue striation spacing analysis", *Materials Characterization*. Vol. 33, (1994), 245-253.
6.   Khan, Z., Rauf, A. and Younas, M., "Prediction of fatigue crack propagation life in notched members under variable amplitude loading", *Journal of Materials Engineering and Performance*. Vol. 6, (1997), 365-373.
7.   Ordico, J. and LeGall, P., "Striation counting on fatigue fractured light alloys", *Reviews Physics Applied*, Vol. 9, (1974), 673-81.
8.   Hershko, E., Mandelker, N., Gheorghiu, G., Sheinkopf, H., Cohen, I. and Levy, O., "Assessment of fatigue striation counting accuracy using high resolution scanning electron microscope", *Engineering Failure Analysis.* Vol. 15, (2008), 20-7.
9.   Hoeppner, D.W. and Krupp, W.E., "Prediction of component life by application of fatigue crack growth knowledge", *Engineering Fracture Mechanics*. Vol. 6, (1974), 47-70.
10. Katsuaki, F., "Method for estimating service load from striation width and height", *Materials Science and Engineering*: *A*. Vol. 285, (2000), 80-84.
11. DeVries, P., Ruth, K. and Dennies, D., "Counting on Fatigue: Striations and Their Measure", *Journal of Failure Analysis and Prevention*. Vol. 10, (2009), 120-137.
12. Yang, J. and Wei, K., "A Statistical Model of Quantitative Relationship between Striation Spacings and Fatigue Crack Growth Rates", *Chinese Journal Metal Science Technology,* Vol. 5, (1989), 407-411.
13. Nedbal, I., Siegl, J., Kunz, J. and Lauschmann, H., "Fractographic reconstitution of fatigue crack history – Part I", *Fatigue & Fracture of Engineering Materials & Structures*. Vol. 31, (2008), 164-176.
14. Nedbal, I., Kunz, J. and Lauschmann, H., "Fractographic reconstitution of fatigue crack history – Part II", *Fatigue & Fracture of Engineering Materials & Structures*. Vol. 31, (2008), 177-183.
15. Troshchenko, V. T. and Prokopenko, A. V., "Fatigue strength of gas turbine compressor blades", *Engineering Failure Analysis*. Vol. 7, (2000), 209-220.
16. Lynch, S. P., "Progression markings, striations, and crack-arrest markings on fracture surfaces", *Materials Science and Engineering*: *A*. Vol. 468, (2007), 74-80.
17. Ruckert, C. O. F. T., Messias Filho, A. A., Bose Filho, W. W., Spinelli, D. and Tarpani, J.R., "Load ratio estimation through striation height and spacing analysis of an aerospace al alloy 7475-T7351", *Journal of Materials Engineering and Performance*. Vol. 20, (2010), 382-389.
18. Schilke, P. W., "Advanced gas turbine materials and coatings", *General Electric*, New York, (2004).
19. Becker, W. T., A.S.M.I.H. Committee and Shipley, R. J., "ASM Handbook: Failure analysis and prevention", ASM International, (2002).
20. Mansur, A., "Modeling of mechanical properties of ceramic-metal composites for armor applications", Ottawa: University of Ottawa; (2011).
21. Bates, R. C. and Clark, W. G., "Fractography and Fracture Mehanics", *Transactions of the American Society for Metals.* Vol. 62, (1969), 380-389.
22. Bakhtyari, H., "Investigation of the causes of GE-F6 gas turbine compressor's 1st row blades failure", Zanjan: University of Zanjan; (2011).

Life Estimate of a Compressor Blade through Fractography

E. Poursaeidi, M. Sanaieei, H. Bakhtyari

Department of Mechanical Engineering, University of Zanjan, Zanjan-45371-38791

چکیده

تحلیل واماندگی قطعاتی که دچار شکست شده‌اند، اطلاعاتی در مورد دلایل و شرایط شکست به دست می‌دهد. فراکتوگرافی بخشی ضروری از تحلیل واماندگی است و در بسیاری از مواقع، تنها راه شناخت مکانیزم شکست است. با استفاده از فراکتوگرافی، می‌توان اطلاعاتی در مورد عمر قطعه و مقادیر ضریب شدت تنش و مقدار تنش وارده به دست آورد. در این مقاله، نتایج بررسی‌های فراکتوگرافی و آنالیز شیمیایی پره‌ی متحرک کمپرسور در یک دستگاه توربین GE Frame 6 ارائه شده است. نتایج بررسی‌ها نشان می‌دهند که منشا ترک، حفرات خوردگی روی سطح پره بوده است. مکانیزم شکست، خستگی با دور بالاست. با استفاده از فاصله‌ی خطوط مواج (striation) عمر قطعه محاسبه و با حل عددی مقایسه شده است. بازه‌ی ضریب شدت تنش و بازه‌ی تنش وارده به قطعه نیز با حل عددی مقایسه شده است. تحلیل‌های فراکتوگرافی و نتایج عددی تطابق قابل قبولی با هم دارند.

doi: *10.5829/idosi.ije.2013.26.04a.08*